Chemical Physics 179 (1994) 455–462
North-Holland

A study of the chemiionization reactions of Ca, Sr and Ba with $O_2(X\,^3\Sigma_g^-)$

A.M. Shaw, J.M. Dyke *
Department of Chemistry, The University, Southampton SO9 5NH, UK

V. Zengin and S. Suzer
Department of Chemistry, Bilkent University, 06533 Ankara, Turkey

Received 23 August 1993

Chemielectron and chemiion spectra resulting from the reactions of effusive beams of Ca, Sr and Ba (in their ground ^1S states) with ground state molecular oxygen $O_2(X\,^3\Sigma_g^-)$ have been recorded using electron spectroscopy and mass spectrometry. The chemielectron spectra are similar for all three reactions exhibiting a strong near-zero energy band and another band at higher electron energies. The chemiion spectra show O_2^+, M^+ and $M_2O_2^+$ as the major ions. The total ion current as well as the individual ion intensities, have been recorded as a function of the extraction potential on the reaction cell. The results obtained indicate that the metal oxide dimer ion is the primary chemiion, formed via an associative ionization reaction of a metal atom with a long-lived metal superoxide intermediate MO_2^*. A two state potential energy curve model is proposed for the $M+MO_2^*$ reaction to explain the shape of the experimental electron distribution.

1. Introduction

Gas-phase reactions of alkaline earth metals play important roles in a number of atmospheric processes and in the chemistry of flames [1,2]. Chemiionization reactions may also be important as primary ionization processes in the ionosphere. Although a number of experimental methods have been used to investigate gas-phase chemiionization reactions of metals with oxidants [3–9], very little use has been made of electron spectroscopy. However, in recent work in this laboratory [10,11], the associative ionization reactions of a number of lanthanide metals with the oxidants $O_2(X\,^3\Sigma_g^-)$, $O_2(a\,^1\Delta_g)$ and $O(^3P)$ have been studied by electron spectroscopy. The spectra obtained, when combined with positive ion mass spectra recorded for the reaction studied, led in each case to identification of the major chemiionization channel and an estimate of its exothermicity. If the simplest metal–oxidant associative ionization reaction is considered,

$$M+O\rightarrow MO^+ + e^- , \qquad (1)$$

then the reaction enthalpy of this reaction can be written as

$$\Delta H_1 = -D_0(MO) + AIE(MO) , \qquad (2)$$

where $D_0(MO)$ and AIE(MO) are the dissociation energy and adiabatic ionization energy of the metal monoxide, MO, respectively. The measured high kinetic energy onset of the experimental electron energy distribution will provide an estimate of ΔH_1, provided that the Franck–Condon factors in the onset region are sufficiently favourable to allow the true onset to be observed experimentally. This approach has been used to estimate the reaction enthalpy of the Sm+O associative ionization reaction and a number of other metal–oxidant chemiionization reactions [10,11]. These studies demonstrated that a metal–oxidant associative ionization reaction will be energetically favoured by the formation of a reaction intermediate with a low ionization energy and a strong metal–oxygen bond. Alkaline earth metals form oxides which satisfy these conditions. However, the

* Corresponding author.

SSDI 0301-0104(93)E0384-8

simple associative ionization reactions of the alkaline earth metals in their ground ^1S states with $O_2(X\,^3\Sigma_g^-)$:

$$M + O_2 \rightarrow MO_2^+ + e^-, \quad (3)$$

can be calculated as strongly endothermic, for M = Ca, Sr or Ba (see table 1). Hence if electrons are detected from the reaction of calcium, strontium or barium with $O_2(X\,^3\Sigma_g^-)$, they cannot arise from this reaction. In the present paper, a study of the chemiionization reactions of these metals in their ground ^1S states with $O_2(X\,^3\Sigma_g^-)$ is reported under effusive beam conditions using electron spectroscopy. Also for each reaction, positive ion mass spectrometry is used to identify the major associative ionization channel.

2. Experimental

Details of the apparatus used in this work have been described briefly elsewhere [10] and a more detailed account is in preparation [12]. A schematic diagram of the ionization chamber of the electron spectrometer used is shown in fig. 1. Electrons produced from a chemiionization reaction were energy analyzed with a hemispherical electrostatic analyzer and the ions produced were mass analyzed using a quadrupole mass spectrometer (SXP 600, VG Quadrupoles).

As shown in fig. 1, ions and electrons were sampled from the *same* reaction cell under a given set of experimental conditions simply by choosing the magnitude and sign of the extraction voltage on the cell. Pulsed radiofrequency induction heating was used to evaporate a metal (Ca, Sr or Ba) from above the reaction cell from molybdenum or tungsten furnaces, to produce metal vapour in the reaction cell. Molecular oxygen ($O_2\,X\,^3\Sigma_g^-$) was added from the side. In a typical experimental study, the partial pressures of the effusive beams of the metal and oxygen in the reaction cell were varied in the range 10^{-5} to 10^{-3} mbar, to investigate the partial pressure dependences of the chemielectron and chemiion signals observed. As described earlier [10,11], a HeI photon source was used to obtain photoelectron spectra from the reaction mixture in order to calibrate the electron energy scale of the chemielectron spectra recorded. The HeI photoelectron spectrum of $O_2(X\,^3\Sigma_g^-)$ proved particularly useful for this.

The electron and ion extraction voltages on the reaction cell were pulsed on a 20 ms duty cycle. The electron extraction voltage (typically −2 V) was applied to the reaction cell in antiphase to the rf heating pulse. In this mode, voltages on the external ion optics of the quadrupole were set to zero. Then during

Table 1
Calculated enthalpies (in eV) for possible $M + O_2(X\,^3\Sigma_g^-)$ reactions

	Ca	Sr	Ba	Equation number in text
$M + O_2 \rightarrow MO_2^+ + e^-$	3.54±0.37	3.24±0.36	0.26±0.93 [a]	3
$M + O_2 \rightarrow MO_2^*$	−2.34±0.17	−2.34±0.26	−5.18±0.83 [b]	4, 5
$2M + O_2 \rightarrow M_2O_2^+ + e^-$	−2.16±0.57	−1.94±0.23	−4.78±0.09 [c]	7
$M + O_2 \rightarrow MO + O$	1.08±0.21	0.84±0.09	−0.51±0.01 [d]	-

[a] Calculated from $D_0^0(M\text{–}O_2)$ and $IE(MO_2)$. $D_0^0(Ba\text{–}O_2) = 5.18 \pm 0.83$ eV [21]. $D_0(Sr\text{–}O_2)$ and $D_0(Ca\text{–}O_2)$ values were taken as those derived in a theoretical study [31] as 2.34±0.26 and 2.34±0.17 eV respectively. $IE(MO_2)$ values were calculated by reducing the known IE(MO) values by the difference in the electron affinities of O^- and O_2^- (1.02 eV) [26,27]. This is reasonable as these oxides are highly ionic [29]. The following values were used for IE(MO): IE(CaO) = 6.90±0.15 eV [28], IE(SrO) = 6.60±0.05 [29] and IE(BaO) = 6.46±0.07 eV [29]. The following values were derived for $IE(MO_2)$: $IE(CaO_2) = 5.88 \pm 0.20$ eV, $IE(SrO_2) = 5.58 \pm 0.10$ eV and $IE(BaO_2) = 5.44 \pm 0.10$ eV.

[b] These values are $-D_0^0(M\text{–}O_2)$ values. They were taken from ref. [21] for $Ba\text{–}O_2$ and ref. [31] for $Ca\text{–}O_2$ and $Sr\text{–}O_2$ (see a)).

[c] Derived overall reaction enthalpy on the assumption that $IE(MO)_2 = IE(MO)$ and $D_0(M\text{–}O_2\text{–}M) = 2D_0(MO)$. Values of IE(MO) and $D_0(MO)$ used are listed in d).

[d] Calculated from $D_0(MO)$ and $D_0(O_2)$ (5.1156 eV) [30]. The $D_0(MO)$ values used are $D_0^0(CaO) = 4.03 \pm 0.21$ eV [24], $D_0^0(SrO) = 4.27 \pm 0.09$ eV [25] and $D_0^0(BaO) = 5.62 \pm 0.01$ eV [22,23].

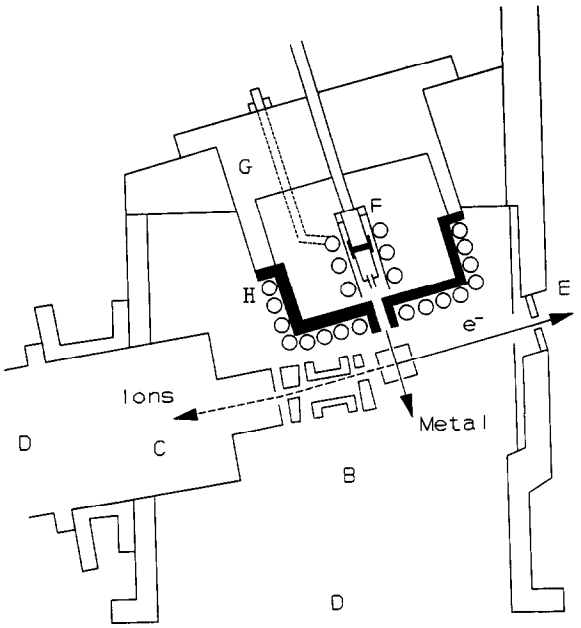

Fig. 1. Schematic diagram of the ionization chamber of the electron spectrometer used for chemiionization studies. In this figure, the following labels are used: (B) extraction optics, (C) quadrupole, (D) diffusion pumps, (E) electron analyzer entrance slits, (F) furnance/radiator assembly, (G) high temperature flange, (H) water cooled shield.

the rf heating pulse, the ion extraction voltage (typically +12 V) was applied to the reaction cell and appropriate voltages set on the external ion optics used to focus ions into the differentially pumped quadrupole mass spectrometer. A gating unit has been designed so that the instrument can be used either for consecutive detection of ions and electrons from the reaction cell under a given set of reaction conditions with extraction voltages pulsed at 50 Hz, or for the detection of only ions or electrons.

For each reaction studied, the dependence of the mass resolved and total ion currents on the voltage applied to the reaction cell has been investigated. Typically, for small applied voltages, inefficient collection of ions occurs. As the voltage increases, the measured total ion current (TIC) increases until a plateau is reached, where the total ion current measured is proportional to the number of chemiions produced in the reaction cell. At higher voltages, a large increase in the total current is observed due to cascade effects [13–15]. This cascade region occurs when the energy of an ion (or electron) gained from the extraction field is above the ionization energy of a reaction component. Under these conditions, two ions may be produced from an ion–molecule reaction. In order to identify primary ions associated with a chemiionization reaction, it is important to perform a voltage dependence study, to identify the plateau region and then record mass spectra in this region. Further details of these ion current characteristics and the mode of operation of this apparatus will be described elsewhere [12].

3. Results and discussion

Chemielectron spectra resulting from the reactions of Ca, Sr and Ba with oxygen at a partial pressure of $\approx 2\times10^{-4}$ mbar are shown in fig. 2. These spectra were recorded at furnace temperatures of 800, 850

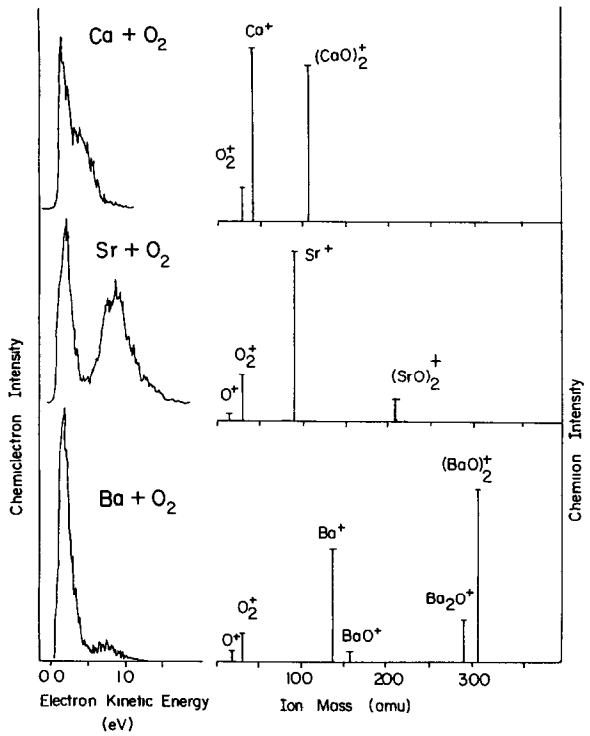

Fig. 2. Chemielectron and chemiion spectra resulting from the reactions of Ca, Sr and Ba with O_2. Typical maximum count rates for the chemielectron spectra are 10^3 c s^{-1}. Typical maximum ion currents recorded in the chemiion spectra are 10^{-11} A.

and 800 K respectively and had typical count rates of 1000 c s^{-1} for the most intense part of each spectrum. In all three cases a strong chemielectron band at nearly zero energy is observed as well as a band at higher energy. For each spectrum, the measured band maxima and high kinetic energy onsets have been listed in table 2. Also shown in fig. 2 are the corresponding mass spectra recorded under the same conditions but with a reaction cell voltage of +15 V. In all cases, the major ions observed are O_2^+, M^+ and $(MO)_2^+$. No $(MO)_2^+$ ions were observed under any experimental conditions.

The result of a typical voltage dependence study on the intensity of the ions observed from the $Ca+O_2$ reaction, recorded at constant reagent partial pressures, is shown in fig. 3. This shows the total ion current (TIC) and the relative ion currents recorded for the metal containing ions, Ca^+ and $(CaO)_2^+$, as a function of reaction cell voltage. As can be seen, the total ion current shows a small plateau followed by a cascade region with an onset at approximately 20 V. The Ca^+ and $(CaO)_2^+$ signals show opposite trends with applied voltage, with the $(CaO)_2^+$ ion decreasing and the Ca^+ ion increasing as the reaction cell voltage increases. In the $Sr+O_2$ case, a similar TIC plot to that shown in fig. 3 was obtained but $(SrO)_2^+$ and Sr^+ show opposite trends to that shown in fig. 3 with the $M_2O_2^+$ ion intensity increasing and the M^+ intensity decreasing as the reaction cell voltage increases. In the $Ba+O_2$ case, a higher $M_2O_2^+ : M^+$ ratio was observed at low voltages on the reaction cell (<15 V) compared to the $Ca+O_2$ case,

Table 2
Electron energy distribution characteristics measured for the $M+O_2(X\,^3\Sigma_g^-)$ reactions [a]

Metal	Band maxima (eV)	High kinetic energy onset (eV)
Ca	0.06	1.10
	0.47	
Sr	0.24	1.60
	0.77	
Ba	0.17	1.31
	0.74	

[a] Experimental error in the tabulated values is ±0.06 eV. As pointed out in the text the experimental high kinetic energy onset in the electron kinetic energy distribution may not be the true onset because of unfavourable Franck–Condon factors.

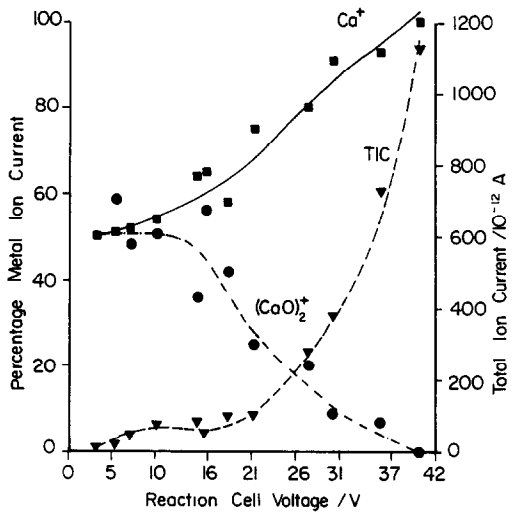

Fig. 3. Dependence of the total ion current (TIC) and relative Ca^+ and $(CaO)_2^+$ ion currents on the reaction cell voltage (see text). The right hand axis (total ion current) refers to the TIC plot; the left hand axis refers to the relative Ca^+ and $(CaO)_2^+$ ion currents.

and BaO^+ and Ba_2O^+ signals were observed. A plateau is observed in the TIC plot as in fig. 3, but the Ba^+ and $Ba_2O_2^+$ signals are approximately constant in the plateau region. To higher voltages of the onset of the cascade, Ba^+ increases and $Ba_2O_2^+$ remains approximately constant. It is clear from these results that although in the plateau region a constant fraction of the total ions are being collected, ion–molecule reactions are occurring which will affect the ratios of the ion signals observed. Possible ion–molecule reactions which could occur in the reaction cell, and hence affect the $M^+ : M_2O_2^+$ ratio, include charge transfer between an ion and a metal atom as this will have the lowest ionization energy of the species in the reaction cell. Most important are reactions of the type $M+(MO)_2^+ \rightarrow M^+ + (MO)_2$, which are endothermic by ≈ 0.2 eV for M=Ca, Sr and Ba, and $M+O_2^+ \rightarrow M^+ + O_2$, which are exothermic by ≈ 6 eV. Also endothermic reactions such as $M^+ + O_2 \rightarrow M+O_2^+$ and $(MO)_2^+ + O_2 \rightarrow (MO)_2 + O_2^+$ with $\Delta H^\phi \approx +6$ eV, will become important as the ions M^+ and $(MO)_2^+$ acquire energy from the reaction cell voltage on leaving the reaction cell.

Evaporation of the alkaline earth metals (Ca, Sr and Ba) from a tungsten or molybdenum furnace un-

der the conditions used produced an effusive beam of the metal atoms. No other species (e.g. metal dimers) are expected to be of significant partial pressures [16] and this was confirmed by photoelectron spectra and electron impact mass spectra recorded under the experimental evaporation conditions. Furthermore, thermal population of electronic excited states of the metals studied at the experimental evaporation temperature is insignificant. Since O_2 is also in its ground state, only ground state reactions should be considered to rationalize the observation of ions and electrons. This should be combined with the main piece of experimental evidence – that the major ions observed are M^+ and $(MO)_2^+$ with no MO_2^+ ions being observed under any experimental conditions. A number of possible chemiionization reactions have been considered and it has been found that all simple bimolecular ionization processes are endothermic for ground state reactants M and O_2. However, collision between a metal atom and an oxygen molecule would lead to a collision complex MO_2^{**} which could be stabilised by collision with a third body to give MO_2^*, an excited metal dioxide with excitation energy less than the dissociation energy $D(M\text{–}O_2)$. If MO_2^* undergoes a collision with a metal atom, an excited dimer $M_2O_2^*$ may be formed with sufficient energy to autoionize.

The following mechanism is therefore proposed to rationalize the observation of chemielectrons and chemiions:

$$M(^1S)+O_2(X\,^3\Sigma_g^-)\rightarrow MO_2^{**}, \quad (4)$$

$$MO_2^{**}+X\rightarrow MO_2^*+X, \quad (5)$$

$$MO_2^*+M(^1S)\rightarrow (MO)_2^*\rightarrow (MO)_2^++e^-, \quad (6)$$

where in this scheme X represents a third body and M a metal atom.

This interpretation means that the observed chemiionization reaction is reaction (6). This would account for the dimer ions observed and the observation of M^+ ions can only be explained in terms of subsequent ion–molecule reactions occurring in the reaction cell.

The overall reaction can be written as

$$2M+O_2\rightarrow M_2O_2^++e^-. \quad (7)$$

Unfortunately, it is not possible to calculate the enthalpies of these reactions, for M = Ca, Sr and Ba, as the necessary heats of formation are not available. However, if the D_{2h} rhomboid structure of Ba_2O_2 with Ba atoms at opposing corners, suggested by infrared matrix isolation studies [17], is assumed for all three M_2O_2 molecules, then it is reasonable to assume that $IE(M_2O_2)=IE(MO)$ and $D_0(M\text{–}O_2\text{–}M)=2D_0(MO)$. These assumptions lead to $\Delta H_7=-2.16\pm0.57$ eV, -1.94 ± 0.23 eV and -4.78 ± 0.09 eV for M = Ca, Sr and Ba respectively. These values can be compared with the experimental high kinetic energy onsets of the electron energy distributions of 1.10, 1.60 and 1.31 eV (see table 2). These two sets of values are not expected to be in good agreement because of the approximations involved in deriving the ΔH_7 values, because deactivation of MO_2^{**} to MO_2^* means that not all the energy of $M\text{–}O_2$ bond formation will be available in the chemiionization process and because the experimental high kinetic energy onset in the electron kinetic energy distribution may not be the true onset because of unfavourable Franck–Condon factors.

The proposed mechanism requires the formation of a long-lived metal superoxide intermediate, MO_2^*, and the formation of a stable dimer ion, $M_2O_2^+$. Some support for these requirements exists in the literature. Metal superoxides of the alkaline earth metals studied in this work have been observed in matrix isolation studies, where the dimer M_2O_2 has been postulated as formed via reaction of the metal with the superoxide [17]. Also, in a recent study of the gas-phase reaction of Ca with N_2O or O_2, optical emission induced by irradiation at 193 nm, was postulated to arise from photolysis of $(CaO)_2$ to produce an excited state of CaO [18]. It has also been noted in refs. [17] and [18] that $(BaO)_2$ is a lot more stable than $(CaO)_2$ and $(SrO)_2$. If this order of stability also applies to their ground state cations, as appears to be the case from the ΔH_7 values listed in table 1, then this would provide some support for observation of $(BaO)_2^+$ as the most intense dimer ion in these $M+O_2$ experiments.

Calcium superoxide, CaO_2, plays an important role in the atmospheric chemistry of calcium [19] and barium superoxide, BaO_2, has been postulated as an intermediate in the $Ba+O_2$ gas-phase reaction, on the basis of the symmetric product angular distribution in the centre of mass frame of the reaction $Ba+O_2\rightarrow BaO+O$ performed under molecular beam

conditions [20]. BaO_2 has also been observed in the gas phase in a crossed-beam study of the reaction $Ba+O_3 \rightarrow BaO_2+O$ [21]. In ref. [21], a value for the $Ba-O_2$ bond energy has been estimated as 5.18 ± 0.83 eV which is lower than the dissociation energy of BaO, 5.62 ± 0.01 eV [22,23].

Having obtained a mechanism for the observed chemiionization reactions which is consistent with the experimental observations, the shape of the electron energy distributions in fig. 2 can be addressed. The collision partners in the ionization process are the internally excited metal superoxide, MO_2^*, and a metal atom in its ground state, $M(^1S)$. The three electron energy distributions shown in fig. 2 are similar in that they show an intense near-zero energy feature as well as a higher energy band. As outlined in the pioneering work of Herman and Cermak [32], and Berry [33], a two state potential energy curve model can be used to rationalize the production of two bands from the $M+MO_2^*$ associative ionization reaction and this is shown schematically in fig. 4. In this figure, the reactants M and MO_2^* approach each other on the initial surface with energy E_1. When the initial and final state potentials become degenerate, there is a finite probability of making a transition to the final state which is controlled by the autoionization width $\Gamma(R)$. This transition is highly localized in the crossing region and produces electrons of near-zero energy with a small spread. If a transition is not made at the crossing point then the reactants proceed to the inner turning point of the initial surface and then make transitions to the vibrational levels of the ionic surface, whose relative intensities are governed by the Franck–Condon factors for the individual transitions. This produces electrons of non-zero energy with a spectral position and width controlled by the difference potential. This simple model would account for the observation of two chemielectron bands.

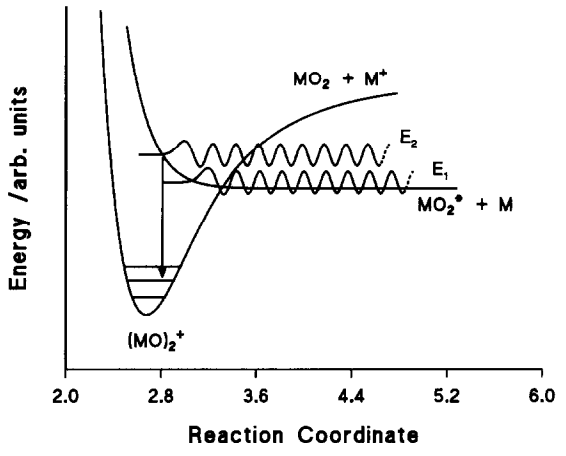

Fig. 4. A schematic two state potential energy curve model for the $M+MO_2^*$ reaction. Ordinate: energy. Abscissa: reaction coordinate.

The probability of making a transition in the region of intersection of the reactant and ionic state potentials depends on the time spent in the crossing region and hence the relative velocity of the reactants. As at a given temperature, the mean velocity is inversely proportional to the square root of the reduced mass of the reactants, $Ca+CaO_2^*$ will have a higher mean velocity than $Ba+BaO_2^*$. Hence the $Ba+BaO_2^*$ reaction is more likely to make a transition in the crossing region than the $Ca+CaO_2^*$ reaction. This is consistent with the dominance of the low energy feature in the $Ba+O_2$ spectrum (see fig. 2).

Increasing the temperature of the furnace, which produces the effusive metal beam, increases the metal vapour pressure and also increases the relative translational energy of the reactants. A higher translational energy in the reactant channel is represented by E_2 in fig. 4. This increase in relative translational energy (from E_1 to E_2) is expected to give rise to a decrease in relative intensity of the zero-energy feature, because the time spent in the crossing region is reduced, and the other chemielectron band will move to slightly higher electron kinetic energy. In practice in the $Ca+O_2$ case, increasing the furnace temperature from 800 to 1100 K had a dramatic effect on the spectrum with almost complete removal of the low energy feature. The effect of furnace temperature on the observed electron distributions for the $Sr+O_2$ and $Ba+O_2$ reactions was less pronounced. In the $Sr+O_2$ case, the high energy feature became approximately equal in height to the low energy band at the highest furnace temperature used (≈ 1100 K) whereas in the $Ba+O_2$ case there was no observable change in the electron energy distribution on increasing the furnace temperature from 800 to 1100 K.

This investigation of the chemiionization reactions of calcium, strontium and barium with $O_2(X\,^3\Sigma_g^-)$ has been extended by studying the chemiionization reactions of these metals with

$O_2(a\,^1\Delta_g)$ and $O(^3P)$ and an account of this work is in preparation [12]. The results obtained support the chemiionization mechanism put forward in this present work for the $M+O_2(X\,^3\Sigma_g^-)$ reactions and show that when oxygen atoms are present in the reaction mixture, the metal suboxide ion (M_2O^+) is a product of another chemiionization reaction.

The chemiionization mechanism in this case can be summarized as follows:

$$M+O\rightarrow MO^{**}, \quad (8)$$

$$MO^{**}+X\rightarrow MO^{*}+X, \quad (9)$$

$$MO^{*}+M\rightarrow M_2O^{+}+e^{-}. \quad (10)$$

In this context, it is notable that BaO^+ and Ba_2O^+ were observed from the $Ba+O_2(X\,^3\Sigma_g^-)$ reaction mixture but no MO^+ and M_2O^+ ions were observed from the $Ca+O_2(X\,^3\Sigma_g^-)$ or $Sr+O_2(X\,^3\Sigma_g^-)$ reactions (see fig. 2). Inspection of table 1 shows that the reaction $M+O_2\rightarrow MO+O$ is endothermic for M = Ca and Sr but exothermic for M = Ba. This implies that the $Ba+O_2(X\,^3\Sigma_g^-)$ reaction is a source of oxygen atoms and probably proceeds with a reasonably high rate at room temperature. This means that, even in the absence of discharged oxygen, reactions (8), (9) and (10) can occur to produce Ba_2O^+. BaO^+ would then be the result of an ion–molecule reaction involving Ba_2O^+ and BaO.

Although the associative ionization reactions responsible for production of ions and electrons from the reaction of Ca, Sr or Ba with O_2 have been deduced in this work, the calculation of reliable enthalpies for the reactions involved has not proved possible because of lack of the necessary thermodynamic values. In particular, this work has highlighted the need for reliable bond energies and first ionization energies for the alkaline earth metal monoxide dimers (M_2O_2) and the alkaline earth dioxides (MO_2). However, as the overall chemiionization process observed in this work is reaction (7), the high kinetic energy onsets of the experimental electron distributions, listed in table 2, can be equated with $\Delta H_7 = -D_0(M\text{–}O_2\text{–}M)+AIE(M_2O_2)$. Clearly, if values for $AIE(M_2O_2)$, for M = Ca, Sr and Ba, can be independently determined then $D_0(M\text{–}O_2\text{–}M)$ values can be derived from the present measurements.

Acknowledgement

This work has been supported by the Air Force Office of Scientific Research (Grant No. AFOSR-89-0351) through the European Office of Aerospace Research (EOARD), United States Air Force and by a NATO Grant (NATO CRG No. 901026). The authors are grateful to Drs. M. Fehér and T. Veszpremi for assistance in the initial stages of this work, and Dr. T.G. Wright for helpful discussions when this manuscript was in preparation.

References

[1] J.M.C. Plane, in: Gas-phase metal reactions, ed. A. Fontijn (Elsevier, Amsterdam, 1992).
[2] J.M. Goodings, in: Gas-phase metal reactions, ed. A. Fontijn (Elsevier, Amsterdam, 1992).
[3] R.H. Burton, J.H. Brophy, C.A. Mims and J. Ross, J. Chem. Phys. 73 (1980) 1612.
[4] T. Mochizuki and K. Lachman, J. Chem. Phys. 65 (1976) 3257.
[5] G.J. Diebold, F. Engelke, H.V. Lee, J.C. Whitehead and R.N. Zare, Chem. Phys. 20 (1977) 265.
[6] R. Haug, G. Rappenecker and C. Schmidt, Chem. Phys. 5 (1974) 255.
[7] R.B. Cohen, C.E. Young and S. Wexler, Chem. Phys. Letters 19 (1973) 99.
[8] H.H. Lo and W.L. Fite, Chem. Phys. Letters 29 (1974) 39.
[9] R.B. Cohen, P. Majeres and J.K. Roloff, Chem. Phys. Letters 31 (1975) 176.
[10] J.M. Dyke, A.M. Shaw and T.G. Wright, Gas-phase metal reactions, ed. A. Fontijn (Elsevier, Amsterdam, 1992).
[11] M.C.R. Cockett, L. Nyulaszi, T. Veszpremi, T.G. Wright and J.M. Dyke, J. Electron Spectry. Relat. Phenom. 57 (1991) 373.
[12] J.M. Dyke, A.M. Shaw and T. Veszpremi, in preparation.
[13] J. Lawton and F.J. Weinberg, Proc. Roy. Soc. A 277 (1964) 468.
[14] T.A. Cool, Appl. Opt. 23 (1984) 1558.
[15] M.P. Gardner, C. Vinkier and K.D. Bayes, Chem. Phys. Letters 31 (1975) 318.
[16] A.N. Nesmeyanov, Vapour pressure of the chemical elements, ed. R. Gary (Elsevier, Amsterdam, 1963).
[17] B.S. Ault and L. Andrews, J. Chem. Phys. 62 (1975) 2312.
[18] J.M.C. Plane and C.F. Nien, J. Chem. Soc. Faraday 87 (1991) 677.
[19] C.F. Nien, B. Rajesekhar and J.M.C. Plane, J. Phys. Chem. 97 (1993) 6449.
[20] P.J. Dagdigian, H.W. Cruse, A. Shultz and R.N. Zare, J. Chem. Phys. 61 (1974) 4450.
[21] H.F. Davis, A.G. Suits, H. Hou and Y.T. Lee, Ber. Bunsenges. Physik. Chem. 94 (1990) 1193.

[22] R.W. Field, J. Chem. Phys. 60 (1974) 2400.
[23] M. Farber and R.D. Srivastava, High Temp. Sci. 7 (1975) 74.
[24] J. Drowart, G. Exsteen and G. Verhaegen, Trans. Faraday Soc. 60 (1964) 1920.
[25] M. Farber and R.D. Srivastava, High Temp. Sci. 8 (1976) 73.
[26] H. Hotop, R.A. Bennett and W.C. Lineberger, J. Chem. Phys. 58 (1973) 2373.
[27] R.J. Celotta, R.A. Bennett, J.L. Hall, M.W. Siegel and J. Levine, Phys. Rev. A 6 (1973) 631.
[28] E. Murad, J. Chem. Phys. 78 (1983) 6611.
[29] J.M. Dyke, M. Feher, B.W.J. Gravenor and A. Morris, J. Phys. Chem. 91 (1987) 4476.
[30] K.P. Huber and G. Herzberg, Molecular spectra and molecular structure, Vol. IV. Constants of diatomic molecules (Van Nostrand, New York, 1979).
[31] C.W. Bauschlicher Jr., H. Partridge, M. Sodupe and S.R. Langhoff, J. Phys. Chem. 96 (1992) 9259.
[32] Z. Herman and V. Cermak, Coll. Czech. Chem. Comm. 31 (1966) 649.
[33] S.E. Niehaus and R.S. Berry, in: Recent progress in mass spectroscopy, eds. K. Ogata and T. Hayakawa (University Park Press, Baltimore, 1970);
R.S. Berry, Advan. Mass Spectrom. 6 (1974) 1.